

# Atom optics hologram in time domain

A. V. Soroko\*

*National Centre of Particle and High Energy Physics, Belarusian State University,  
Bogdanovich Street 153, Minsk 220040, Belarus*

A temporal evolution of atomic wave packet interacting with object and reference electromagnetic waves is investigated beyond the linear respond. Under this condition the diffraction of ultracold atomic beam on inhomogeneous laser radiation is interpreted as beam's passing through a three-dimensional hologram, which thickness is proportional to the interaction time. It is shown that diffraction efficiency of such a hologram may reach 100% and is determined by the time domain.

03.75.Be, 42.50.Vk, 32.80.Lg, 81.15.Fg

## I. INTRODUCTION

The achievements of the last decade in the field of laser light cooling below the recoil limit [1,2] have opened a new chapter of atom optics which objective is to manipulate atomic beams in a way similar to conventional optics by exploiting the wave properties of the particles. Indeed, if momenta of cooled atoms verge to the photon ones, diffraction effects may manifest themselves especially strongly during atomic interaction with space inhomogeneous radiation. For the corresponding part of the de Broglie wave spectrum, this provides a possibility of supplementing the traditional atom optics set of elements such as mirrors [3], diffraction gratings [4,5] or lenses [6] with holograms of different objects, the conventional optics analogues of which have been well known for several decades [7]. The destination of such atomic holograms is to create matter waves with intended amplitude and phase characteristics. Since these characteristics are the same as for the object wave one obtains a strong and convenient implement for holographic imaging with atoms. The latter may have useful practical applications from atom lithography [8] to the manufacturing of microstructures, or quantum microfabrication.

One of possibilities to make atomic hologram consists in creation a mechanical mask with appropriate transparency for the incident atomic beam (analogue of two-dimensional optical hologram). Such a hologram has the advantage of being permanent, however, up to now only the masks with binary transparency have been prepared. So in the experiment [9] the mask was written onto a thin silicon nitride membrane and allowed for complete or vanishing transmission of the beam at a given point. Evidently this reduces resolution in the reconstructed image, because correct holographic storage of information requires the gradually varying transmission of the beam.

Very interesting proposal has recently been reported in the work [10], where the authors suggest to use a Bose-Einstein condensate (BEC) as a registration media for atomic hologram. It illustrates the wide potential applicability of condensates which after having been realized experimentally [11] are available almost routinely in several laboratories. In this method desired information is encoded into the condensate in the form of density modulations by using object and reference laser beams that form writing optical potential. The reconstruction of matter wave arises due to s-wave scattering of the reading-beam atoms on condensate inhomogeneities.

In the previous paper [12] we have shown that atomic hologram may also be constructed (at certain conditions) as a superposition of reference and object electromagnetic waves to be common for optical holography. The creation of intended matter wave arises when ultracold atomic beam is diffracted from this hologram which in a fact represents itself the inhomogeneous light field. Main advantages of the proposed scheme are it's simplicity because of skipping the recording process and, as a consequence, absence of aberrations in the stored information. In some sense our approach is close to the non-holographic scheme of wave front engineering [13], which implies to arbitrarily shape the center-of-mass wave function of an atom by means of a sequence of suitably shaped laser pulses, because both methods are based only on atom-laser interactions.

Main assumption being employed in our holographic scheme is the linear respond of atomic system on the laser-field inhomogeneity. It requires, in particular, the weak perturbation of the incident atomic beam and sets an upper limit on the object wave amplitude (see Eq. (50) in the Ref. [12]). As a result only a little part of atoms in the beam can be transferred into the reconstructed matter wave. Linear respond operation decreases the diffraction efficiency of an atomic hologram, i.e. the ratio of the intensity of diffracted atomic waves to the intensity of reading beam, what may be crucial for practical applications. In conventional optical holography such a situation corresponds to the kinematical regime of writing information [7]. On the other hand, the coupled wave theory of Kogelnik [14] and the theories based on dynamical approximation [15–17], give one a recipe how to create a hologram with high (up to 100%) diffraction efficiency. In this purpose it is necessary to control, besides others, such a parameter as the thickness of the hologram. Unfortunately the thickness control is difficult to perform in the scheme of atom holography without registration medium like our one (see Figure 1 for details). So

the purpose of present paper is to suggest a new approach for creation of atom optics holograms which will inherit the advantages of our previous scheme and also allow high diffraction efficiencies. We will show that desired approach can be realized if one restricts the existence of atomic hologram rather in a time than space domain, so that the hologram will work in a pulsed regime pumping atoms from the beam or initial wave packet into the reconstructed wave. Note that suggested regime is well compatible with the Raman cooling methods [2] (including laser cooling below the gravitational limit [18]) and the recent realization of an atom laser [23], which in a fact repeatedly reproduce coherent or almost coherent atomic wave packets necessary for actual implementation of a reading beam.

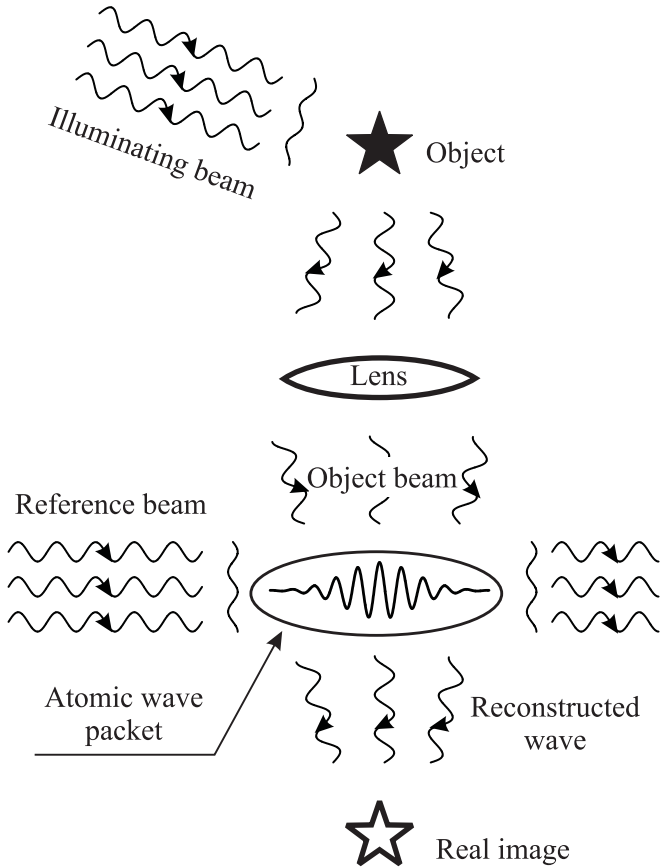


FIG. 1. Typical for atomic holography layout design of laser beams and matter wave packets.

Another important prerequisite for successful wave-front reconstruction with massive particles concerns the compensation for potentially detrimental influence of gravitational effects. Fortunately, the bulk of atoms has the magnetic moment, and all one has to do is use the Stern-Gerlach effect. Superimposing the weakly inhomogeneous magnetic field onto the path of prepolarized particles and appropriately adjusting the field gradient, it is possible to suspend the ground state atoms everywhere

except the region of interaction with radiation. But if the laser frequency is far from all atom transitions, the contribution to the total force induced by spatially dependent shifts of the Zeeman levels is negligible. Under this condition, atoms move like free particles being affected only by the electromagnetic waves.

In Sec. II we derive a system of equations which describe interaction of atomic wave packet with object and reference electromagnetic waves when the gravity is compensated. Approximate solution of this system is found not assuming weak perturbation of initial state, and domain of its validity is determined. For reasonable experimental conditions the solution admits an atom-optics interpretation that is done in Sec. III. Namely, the inhomogeneous laser radiation is shown to behave like a three-dimensional hologram in respect to the impinging wave packets. A numerical simulation of such a hologram created with 31-mode object beam is presented, and high diffraction efficiency is demonstrated. Section IV concludes with a summary of the obtained results. Most cumbersome expressions are placed into Appendix.

## II. BASIC FORMULAS

### A. Compensation for the gravity

Consider for definiteness an atom with a  $J = \frac{1}{2}$  to  $J = \frac{3}{2}$  transition, e.g., sodium or cesium. The magnetic field  $\mathbf{B}(\mathbf{r})$  applied to compensate for the gravity is supposed to contain a homogeneous component  $\mathbf{B}_0$  directed along the gravity acceleration  $\mathbf{B}_0 \uparrow\uparrow \mathbf{g}$ . The remaining inhomogeneous part of the field  $\mathbf{B}_1(\mathbf{r}) = \mathbf{B}(\mathbf{r}) - \mathbf{B}_0$  should be small compared to this component

$$|\mathbf{B}_1(\mathbf{r})| \ll B_0 = |\mathbf{B}_0|. \quad (2.1)$$

As we will see below, to fulfil this condition it is necessary to take  $B_0$  in the range  $10^3 \div 10^4$  G. In practice such a field is strong enough to induce Zeeman shifts which considerably exceed the hyperfine splitting intervals  $\sim \hbar\omega_{\text{HFS}}$  (but not the multiplet ones). Therefore an internal atomic eigenstate  $|J, I, M_J, m_I\rangle$  may be well described using the set of quantum numbers consisting of the angular momenta of electronic shell  $J$  and nucleus  $I$ , and their local projections  $M_J, m_I$ , on the direction of the magnetic field. The corresponding energy eigenvalue is determined not only by the multiplet level  $E_J$  but also by the magnetic field  $B(\mathbf{r}) = |\mathbf{B}(\mathbf{r})|$  and therefore is spatially dependent

$$E_{|J, I, M_J, m_I\rangle}(\mathbf{r}) = E_J + aM_Jm_I + (\mu_B g_L M_J - \mu_{\text{nuc}} m_I)B(\mathbf{r}), \quad (2.2)$$

where  $a$  is the hyperfine coupling constant ( $a \propto \hbar\omega_{\text{HFS}}$ , e.g., for Na  $a/\hbar = 885.8$  MHz),  $g_L$  denotes the Lande factor, and  $\mu_{\text{nuc}}$  is the nuclear magnetic moment. Because of condition (2.1) such a spatial dependence, however, mainly arises from the longitudinal ( $B_1^{\parallel}(\mathbf{r}) = \mathbf{B}_0 \cdot$

$\mathbf{B}_1(\mathbf{r})/B_0$ ), rather than the transverse ( $\mathbf{B}_1^\perp(\mathbf{r})$ ) component of the vector  $\mathbf{B}_1(\mathbf{r})$ , provided that the components are defined relative to  $\mathbf{B}_0$ . This is evident from the expression

$$B(\mathbf{r}) = \sqrt{\left[B_0 + B_1^\parallel(\mathbf{r})\right]^2 + \left[\mathbf{B}_1^\perp(\mathbf{r})\right]^2} \simeq B_0 + B_1^\parallel(\mathbf{r}) + \left[\mathbf{B}_1^\perp(\mathbf{r})\right]^2/(2B_0), \quad (2.3)$$

where the term containing  $\mathbf{B}_1^\perp(\mathbf{r})$  is small and can be neglected. Consequently, by adjusting the gradient of the field  $B_1^\parallel(\mathbf{r})$  one can achieve translation invariance of the ground state  $|g\rangle = |1/2, I, -1/2, I\rangle$  (or another state with  $J = 1/2$ ) in three dimensions:

$$E_{|g\rangle}(\mathbf{r}) - Mg \cdot \mathbf{r} = \text{const.} \quad (2.4)$$

For example, to balance the gravitational force in this way for sodium it is necessary to create a gradient  $\nabla B_1^\parallel(\mathbf{r}) = b_1 \mathbf{g}/|\mathbf{g}|$ , where  $b_1 = -4.033$  G/cm. This condition does not contradict the Maxwell equation  $\nabla \cdot \mathbf{B}_1(\mathbf{r}) = 0$ , because variation of  $\mathbf{B}_1^\perp(\mathbf{r})$  is not restricted. Note also that the choice  $B_0 = 10^3 \div 10^4$  G maintains condition (2.1) very well within a spatial region of the size  $\sim 10$  cm.

All the other levels are affected by the residual external potential. In particular, the force  $\mathbf{f}_e$  acting on the atoms in the excited state, e.g.,  $|e\rangle = |3/2, I, -3/2, I\rangle$ , may be estimated from Eqs. (2.2) and (2.4) as  $|\mathbf{f}_e| \sim Mg$ .

## B. Interaction with laser beams

In our scheme, we use pulses of laser light at frequency  $\omega$  which is roughly tuned to the  $|g\rangle \rightarrow |e\rangle$  transition. If the typical size  $2L$  of atomic sample is restricted by the condition  $L \ll a/(Mg)$ , one may regard  $E_{|e\rangle}(\mathbf{r})$  as the closest to resonance excited level within the whole interaction domain. Indeed, the maximal spatial shift of the level  $\sim MgL$  induced by the force  $\mathbf{f}_e$  appears to be much less than the hyperfine splitting intervals ( $MgL \ll a \sim \hbar\omega_{\text{HFS}}$ ), and the hierarchy of detunings retains. Therefore an atom initially in  $|g\rangle$  state behaves as a two-level system with respect to the processes with stimulated emission of photons.

Each laser beam is considered as a discrete superposition of plane monochromatic electromagnetic waves. In particular, we use the following decomposition of the electric field in the object beam

$$\mathbf{E}_s(\mathbf{r}, t) = \sum_{m \geq 1} \mathbf{E}_m \exp(i\mathbf{k}_m \cdot \mathbf{r} - i\omega t) + \text{c.c.}, \quad (2.5)$$

where  $\mathbf{E}_m$  and  $\mathbf{k}_m$  stand for the complex amplitude of the mode  $m$  and its wave vector respectively. Such an approach, does not somehow restrict the generality of consideration, because in our experimental setup atom

moves inside a superposition of reference and object laser beams during all the interaction time, and the expression (2.5) must well describe the real laser field only in the atom-laser interaction region. Evidently, the latter requirement can always be satisfied by decreasing the minimal angle between the mode wave vectors. In this case we can also regard the reference beam as a single mode (with the index  $m = 0$ )

$$\mathbf{E}_r(\mathbf{r}, t) = \mathbf{E}_0 \exp(i\mathbf{k}_0 \cdot \mathbf{r} - i\omega t) + \text{c.c.}, \quad (2.6)$$

which is a typical arrangement for optical holography.

Since the atomic dipole momentum operator  $\hat{\mathbf{d}}$  is diagonal in quantum numbers  $I$  and  $m_I$ , the transitions which change  $m_I$  are allowed only due to hyperfine interaction. As a consequence, the excited state  $|e\rangle$  decays to the lower ones preferentially in the channel  $|e\rangle \rightarrow |g\rangle$  (with the rate  $\gamma$ ). This circumstance makes it possible to deal with an atom as a two-level system even if spontaneous photon emission takes place. However, to simplify the consideration the coherent scattering processes are assumed to dominate the spontaneous emission, i.e., the regime  $|\Delta| \gg \gamma$  is kept [20,21], where  $\Delta = \omega + [E_{|g\rangle}(0) - E_{|e\rangle}(0)]/\hbar$  is the detuning from resonance in the center of atom-laser interaction region ( $\mathbf{r} = 0$ ). Under such a condition the one-particle density matrix in momentum representation [22] has an obvious time evolution

$$\rho_{ab}(\mathbf{p}_1, \mathbf{p}_2, t) = \int d\mathbf{p}'_1 \int d\mathbf{p}'_2 \sum_{a'b'} G_{aa'}(\mathbf{p}_1, \mathbf{p}'_1, t) \times G_{bb'}^*(\mathbf{p}_2, \mathbf{p}'_2, t) \rho_{a'b'}(\mathbf{p}'_1, \mathbf{p}'_2, t = 0), \quad (2.7)$$

where indices  $a, b \dots$  span the internal atomic states ( $e, g$ ) and  $G_{aa'}(\mathbf{p}_1, \mathbf{p}'_1, t)$  is the Green function of two-component Shrödinger equation describing atomic dynamics during the  $|g\rangle \leftrightarrow |e\rangle$  transitions.

In rotating wave approximation this equation rewritten for slowly time dependent ground- and excited-level wave functions  $\psi_g(\mathbf{p}, t)$  and  $\psi_e(\mathbf{p}, t)$  takes the form

$$i \frac{\partial}{\partial t} \psi_g(\mathbf{p}, t) = [t(\mathbf{p}) + \Delta] \psi_g(\mathbf{p}, t) - \sum_{m \geq 0} \Omega_m^* \psi_e(\mathbf{p} + \hbar\mathbf{k}_m, t), \quad (2.8a)$$

$$i \frac{\partial}{\partial t} \psi_e(\mathbf{p}, t) = [t(\mathbf{p}) - i\mathbf{f}_e \cdot \nabla] \psi_e(\mathbf{p}, t) - \sum_{m \geq 0} \Omega_m \psi_g(\mathbf{p} - \hbar\mathbf{k}_m, t), \quad (2.8b)$$

where  $\Omega_m = \langle e | \hat{\mathbf{d}} \cdot \mathbf{E}_m | g \rangle / \hbar$  is the Rabi frequency of mode  $m$ , and the terms  $t(\mathbf{p}) = \mathbf{p}^2/(2M\hbar)$  and  $-i\mathbf{f}_e \cdot \nabla$  arise in momentum space from the kinetic and potential energy  $(-\mathbf{f}_e \cdot \mathbf{r})$  correspondingly.

For the situation at hand, the upper electronic state can be adiabatically eliminated from Eqs. (2.8) provided that the detuning  $\Delta$  is large enough [5,20]

$$|\Delta| \gg |\Omega_m|, |\mathbf{f}_e|L/\hbar. \quad (2.9)$$

The route by which one can do it implies a self-consistent assumption  $|\psi_e| \ll |\psi_g|$  leading to the zero-order solution of the Eq. (2.8a):  $\psi_g(\mathbf{p}, t) \simeq \exp\{-i[t(\mathbf{p}) + \Delta]t\}\psi_g(\mathbf{p}, t = 0)$ . After substitution of this expression into Eq. (2.8b) the latter may be solved in the framework of perturbation theory developed in respect to the potential energy term. In this case, the excited-level wave function acquires a representation

$$\psi_e(\mathbf{p}, t) \simeq - \sum_{m \geq 0} \frac{\Omega_m \psi_g(\mathbf{p} - \hbar\mathbf{k}_m, t)}{t(\mathbf{p}) - t(\mathbf{p} - \hbar\mathbf{k}_m) - \Delta} + \dots, \quad (2.10)$$

where the dots denote omitted terms which include a small ( $\propto |\mathbf{f}_e|L/|\hbar\Delta|$ ) first-order correction to  $\psi_e(\mathbf{p}, t)$  and also summands which oscillate with the non-resonant frequency  $t(\mathbf{p})$  and therefore give a negligible contribution when one uses above expression within the context of Eq. (2.8a).

For ultracold atomic sample one can further discard the kinetic energy terms in denominators of the expression (2.10). As a result the motion of the ground-state atom is described with the equation

$$\begin{aligned} i \frac{\partial}{\partial t} \psi_g(\mathbf{p}, t) &= [t(\mathbf{p}) + \Delta + f_0] \psi_g(\mathbf{p}, t) \\ &+ \sum_{m \geq 1} \left\{ \sum_{\substack{n \geq 1 \\ n \neq m}} f_{mn} \psi_g[\mathbf{p} - \hbar(\mathbf{k}_m - \mathbf{k}_n), t] \right. \\ &+ g_m \psi_g[\mathbf{p} - \hbar(\mathbf{k}_m - \mathbf{k}_0), t] \\ &\left. + g_m^* \psi_g[\mathbf{p} + \hbar(\mathbf{k}_m - \mathbf{k}_0), t] \right\}, \end{aligned} \quad (2.11)$$

where

$$f_0 = \frac{1}{\Delta} \sum_{m \geq 0} |\Omega_m|^2, \quad (2.12)$$

$$f_{mn} = \frac{\Omega_m \Omega_n^*}{\Delta}, \quad (2.13)$$

and

$$g_m = \frac{\Omega_m \Omega_0^*}{\Delta} \quad (2.14)$$

stand for the effective Rabi frequencies.

### C. Evolution of wave packets

It is known from the theory of thick optical holograms that reconstruction of the original (conjugate) object wave arises only if the reading beam is directed along (opposite) the reference wave and has the same wavelength. Relying on analogy with conventional optics let us consider for definiteness the evolution of atomic wave

packet whose spectrum is initially concentrated around the mean momentum of photons in the reference beam. In such a case one can anticipate creation of the matter wave being similar to the forward object wave. Therefore it is convenient to look for the solution of Eq. (2.11) as a sum of wave packets approaching the plane modes of hologram [16]

$$\psi_g(\mathbf{p}, t) = \sum_{m \geq 0} \psi_m(\mathbf{p} - \hbar\mathbf{k}_m, t). \quad (2.15)$$

Initially there are no wave packets corresponding to the object beam, so that

$$\psi_m(\mathbf{p}, t = 0) = 0, \quad m \geq 1, \quad (2.16)$$

and as a consequence

$$\psi_0(\mathbf{p} - \hbar\mathbf{k}_0, t = 0) = \psi_g(\mathbf{p}, t = 0) \equiv \psi_g(\mathbf{p}). \quad (2.17)$$

Population of these atomic motional states ( $m \geq 1$ ) arises due to coupling with  $\psi_0(\mathbf{p}, t)$ , the wave packet corresponding to the reference beam:

$$i \frac{\partial}{\partial t} \psi_m(\mathbf{p}, t) = t_m(\mathbf{p}) \psi_m(\mathbf{p}, t) + g_m \psi_0(\mathbf{p}, t), \quad (2.18)$$

where

$$t_m(\mathbf{p}) = t(\mathbf{p} + \hbar\mathbf{k}_m) + \Delta + f_0. \quad (2.19)$$

Depletion of the state with  $m = 0$  is governed by the equation

$$i \frac{\partial}{\partial t} \psi_0(\mathbf{p}, t) = t_0(\mathbf{p}) \psi_0(\mathbf{p}, t) + \sum_{m \geq 1} g_m^* \psi_m(\mathbf{p}, t) + \chi(\mathbf{p}, t), \quad (2.20)$$

which one can obtain after substituting Eqs. (2.15), (2.18) into Eq. (2.11).

So we bring the Eq. (2.11) to the system of equations (2.18), (2.20). The advantage of such a step becomes obvious after making a self-consistent assumption about momentum spectrum of  $\psi_m(\mathbf{p}, t)$ ,  $m \geq 0$ , the validity of which was verified for two-mode case in Ref. [18]. Namely, we will suppose below that all non-vanishing functions have narrow distributions around  $\mathbf{p} = 0$  and, as a result, do not overlap in the expression for  $\chi(\mathbf{p}, t)$

$$\begin{aligned} \chi(\mathbf{p}, t) &= \sum_{m \geq 1} \left\{ \sum_{n \geq 1} g_n \psi_m[\mathbf{p} + \hbar(2\mathbf{k}_0 - \mathbf{k}_n - \mathbf{k}_m), t] \right. \\ &+ \sum_{\substack{n \geq 0 \\ n \neq m}} g_m^* \psi_n[\mathbf{p} + \hbar(\mathbf{k}_m - \mathbf{k}_n), t] \\ &+ \sum_{n \geq 1} \sum_{l \geq 0} f_{mn} \\ &\left. \times \psi_l[\mathbf{p} + \hbar(\mathbf{k}_0 - \mathbf{k}_l - \mathbf{k}_m + \mathbf{k}_n), t] \right\}. \end{aligned} \quad (2.21)$$

In such circumstances different parts of this term give incoherent contributions, which appear to be small at low  $g_m$  and can be taken into account within the theory of perturbation. In zero-order approximation one omits  $\chi(\mathbf{p}, t)$  so that the system (2.18), (2.20) becomes homomorphic with the rate equations describing a  $(m+1)$ -level atom. Note, the stationary solutions of this truncated system exactly coincide with eigenmodes of corresponding optical hologram [16].

To go further it is convenient to perform the Laplace transformation ( $m \geq 0$ )

$$\psi_m(\mathbf{p}, \lambda) = \int_0^\infty dt e^{-\lambda t} \psi_m(\mathbf{p}, t) \quad (2.22)$$

with the initial conditions (2.16), (2.17). Then the equations for the Laplace transforms will allow an easy zero-order solution

$$\psi_0^{(0)}(\mathbf{p}, \lambda) = \frac{-i}{T(\mathbf{p}, \lambda)} \psi_g(\mathbf{p} + \hbar \mathbf{k}_0), \quad (2.23a)$$

$$\psi_m^{(0)}(\mathbf{p}, \lambda) = \frac{-g_m}{t_m(\mathbf{p}) - i\lambda} \psi_0^{(0)}(\mathbf{p}, \lambda), \quad m \geq 1, \quad (2.23b)$$

where

$$T(\mathbf{p}, \lambda) = t_0(\mathbf{p}) - i\lambda + \sum_{m \geq 1} \frac{-|g_m|^2}{t_m(\mathbf{p}) - i\lambda}. \quad (2.24)$$

Similarly, next iteration reproduces the first-order solution

$$\psi_0^{(1)}(\mathbf{p}, \lambda) = \psi_0^{(0)}(\mathbf{p}, \lambda) + \frac{-\chi^{(0)}(\mathbf{p}, \lambda)}{T(\mathbf{p}, \lambda)}, \quad (2.25a)$$

$$\psi_m^{(1)}(\mathbf{p}, \lambda) = \frac{-g_m}{t_m(\mathbf{p}) - i\lambda} \psi_0^{(1)}(\mathbf{p}, \lambda), \quad m \geq 1, \quad (2.25b)$$

where  $\chi^{(0)}(\mathbf{p}, \lambda)$  is obtained from the expression (2.21) after making the substitutions  $\psi_m(\mathbf{p}, t) \rightarrow \psi_m^{(0)}(\mathbf{p}, \lambda)$ ,  $m \geq 0$ . In principle, we can get the solution with any preassigned accuracy by repeating the iterations but it will be sufficient to restrict ourselves to the first-order formulas for the following consideration.

Desired time-dependent wave functions arise then as the inverse Laplace transforms of  $\psi_m(\mathbf{p}, \lambda)$  in agreement with the Mellin formula

$$\psi_m(\mathbf{p}, t) = 2\pi i \int_{\epsilon-i\infty}^{\epsilon+i\infty} d\lambda e^{\lambda t} \psi_m(\mathbf{p}, \lambda), \quad \epsilon > 0. \quad (2.26)$$

Finally, using the Eqs. (2.25) and (2.26) one can easily write down an expression for the ground-state component  $G_{gg}(\mathbf{p}, \mathbf{p}', t)$  of the Green function appearing in the formula (2.7). We placed this expression into the Appendix.

## D. Validity of the solution

At first let us check that the zero-order solution (2.23) indeed has a narrow momentum spectrum around  $\mathbf{p} = 0$ , provided the initial conditions are chosen properly, and the effective Rabi frequency  $g_m$  is small enough. Doing it we may restrict ourselves to examination of only a region  $\mathcal{D} = \{\mathbf{p} : |t_m(\mathbf{p}) - t_0(\mathbf{p})|^2 \lesssim |g_m|^2, \forall m\}$ , where all the functions in truncated system of equations (2.18), (2.20) have a possibility to influence each other resonantly. In this region one can identify the kinetic-energy terms  $t_m(\mathbf{p})$  related to different modes of the object beam ( $m \geq 1$ ) without any damage for the result of estimation:  $t_m(\mathbf{p}) \approx t_n(\mathbf{p}) \approx \tilde{t}(\mathbf{p})$ , where  $\tilde{t}(\mathbf{p}) = t(\mathbf{p} + \hbar \tilde{\mathbf{k}}) + \Delta + f_0$ , and  $\tilde{\mathbf{k}}$  is some typical wave vector in the object beam. Under this condition the integral in the Eq. (2.26) can be calculated explicitly, and the wave functions  $\psi_m^{(0)}(\mathbf{p}, t)$  get a simple analytical representation

$$\psi_0^{(0)}(\mathbf{p}, t) \simeq A_r(\mathbf{p}, t) e^{-ib(\mathbf{p})t} \psi_g(\mathbf{p} + \hbar \mathbf{k}_0), \quad (2.27a)$$

$$\psi_m^{(0)}(\mathbf{p}, t) \simeq A_s(\mathbf{p}, t) \frac{g_m}{g_\Sigma} e^{-ib(\mathbf{p})t} \psi_g(\mathbf{p} + \hbar \mathbf{k}_0), \quad m \geq 1. \quad (2.27b)$$

In these formulas

$$A_r(\mathbf{p}, t) = \frac{ia(\mathbf{p})}{d(\mathbf{p})} \sin[d(\mathbf{p})t] + \cos[d(\mathbf{p})t], \quad (2.28a)$$

$$A_s(\mathbf{p}, t) = \frac{-ig_\Sigma}{d(\mathbf{p})} \sin[d(\mathbf{p})t], \quad (2.28b)$$

where

$$a(\mathbf{p}) = [\tilde{t}(\mathbf{p}) - t_0(\mathbf{p})]/2, \quad (2.29)$$

$$b(\mathbf{p}) = a(\mathbf{p}) + t_0(\mathbf{p}), \quad (2.30)$$

$$d(\mathbf{p}) = \sqrt{a(\mathbf{p})^2 + g_\Sigma^2}, \quad (2.31)$$

and

$$g_\Sigma = \left( \sum_{m \geq 1} |g_m|^2 \right)^{1/2} \quad (2.32)$$

stands for the overall effective Rabi frequency.

It is seen from Eqs. (2.27) that initial atomic wave packet transforms into motional states with  $m \geq 1$  at a time  $\tau_n$  (time of the  $n\pi$  pulse [21])

$$\tau_n = \frac{\pi}{2g_\Sigma} (2n - 1), \quad n \in \mathcal{N}. \quad (2.33)$$

This transition is velocity-selective with the most efficiency determined by the Bragg resonance condition  $\mathbf{p} \cdot \Delta_k = 0$ , where  $\Delta_k = (\tilde{\mathbf{k}} - \mathbf{k}_0)$  denotes a typical difference between wave vectors in the object and reference beams (cf. Ref. [20]). The width of a peak in momentum distribution along the direction of vector  $\Delta_k$  (the interval from maximum to the first minimum) depends on interaction time, and for  $t \leq 2\tau_1$  is

$$\delta_p(t) = \frac{2Mg_\Sigma}{\Delta_k} \sqrt{4\left(\frac{\tau_1}{t}\right) - 1}. \quad (2.34)$$

For given value  $\Delta_k = |\Delta_k|$  it decreases with  $g_\Sigma$ . Therefore the smaller the effective Rabi frequencies  $g_m$  the narrower the momentum spectrum of  $\psi_m^{(0)}(\mathbf{p}, t)$ .

Evidently, to prevent all non-vanishing functions composing the term  $\chi(\mathbf{p}, t)$  from being overlapped in momentum space their spectra must be concentrated within the domain  $|\mathbf{p}| < \hbar\delta_k$  at  $t \sim \tau_1$ , where

$$\delta_k = \min_{m,n \geq 0} |\mathbf{k}_m - \mathbf{k}_n| \quad (2.35)$$

is the minimal distance between different wave vectors of the laser beams (see Figure 2).

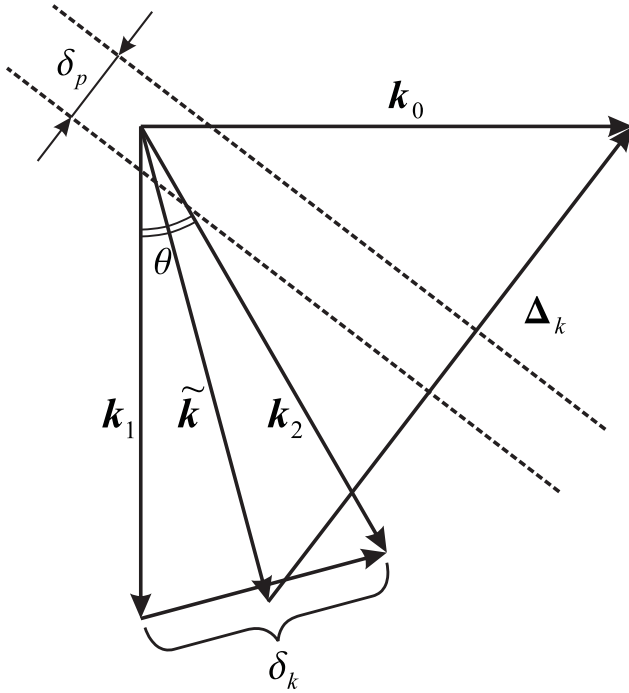


FIG. 2. Definitions of the values  $\Delta_k$ ,  $\delta_k$ , and  $\delta_p$  in the simplest case of two-mode object wave.

Since the spectral extent along the direction of vector  $\Delta_k$  is characterized by  $\delta_p(t)$ , we immediately get the first of sufficient conditions

$$\delta_p(\tau_1) \ll \hbar\delta_k. \quad (2.36)$$

In agreement with the Eq. (2.34) it sets an upper limit on the overall effective Rabi frequency

$$g_\Sigma \ll \hbar\delta_k\Delta_k/(2\sqrt{3}M). \quad (2.37)$$

In the transverse direction the spectra are the same as that of initial wave packet  $\psi_g(\mathbf{p} + \hbar\mathbf{k}_0)$ . Therefore one must impose another condition

$$|(\mathbf{p}' - \hbar\mathbf{k}_0) \times \Delta_k| < \hbar\delta_k\Delta_k, \quad (2.38)$$

which restricts allowed values of  $\mathbf{p}'$  in the domain of the Green function  $G_{gg}(\mathbf{p}, \mathbf{p}', t)$ .

When the inequalities (2.36), (2.38) are met, the main correction to the zero-order solution  $\psi_m^{(0)}(\mathbf{p}, t)$  caused by the term  $\chi(\mathbf{p}, t)$  arises outside the near-resonance region  $\mathcal{D}$  and depends on geometry of laser beams. So for  $t \sim \tau_1$  and 2D holographic setup like that in the Fig. 2 (i.e., all  $\mathbf{k}_m$  are coplanar vectors) the relative correction has the order of magnitude  $\varepsilon_r = \delta_p(\tau_1)/(\hbar\delta_k) \ll 1$ , what can be seen from Eqs. (2.21), (2.27b). Note, while making this estimation we discarded the third summand in the expression (2.21), because it is proportional to  $f_{mn}$  and, consequently, is much less than the first and second ones ( $\propto |g_m|$ ), provided the standard holographic restriction on the intensities of laser beams  $|\mathbf{E}_0|^2 \gg |\mathbf{E}_m|^2$ ,  $m \geq 1$ , leading to the inequality  $|g_m| \gg |f_{mn}|$ , is applied here.

To illustrate the said in the case of two-mode object wave let us regard absolute values of zero-order solution  $|\psi_g^{(0)}|$  and first-order correction to it  $\delta^{(0)} = |\psi_g^{(1)} - \psi_g^{(0)}|$  as functions of the momentum component  $p_x$  and the angle  $\theta$  between  $\mathbf{k}_1$  and  $\mathbf{k}_2$ , assuming a Cartesian coordinate system is introduced in momentum space,  $\mathbf{p} = (p_x, p_y, p_z)$ , with  $x$  ( $y$ ) axis chosen along (opposite) the vector  $\mathbf{k}_0$  ( $\mathbf{k}_1$ ). Figure 3 shows corresponding dependences after  $\pi$ -pulse time calculated for sodium atoms, provided the initial wave packet has the Gaussian profile  $\psi_g(\mathbf{p}) \propto \exp[-L^2(\mathbf{p} - \mathbf{p}_0)^2/(2\hbar^2)]$  with mean momentum  $\mathbf{p}_0 = \hbar\mathbf{k}_0$ ,  $|\mathbf{k}_0| = k_0 = 1.07 \times 10^5 \text{ cm}^{-1}$ , spatial extension  $2L = 0.4 \text{ cm}$ , and 2D norm equal to 1. The peaks in central region of each plot correspond to forbidden values of  $\theta \propto \delta_k < \delta_p(\tau_1)$ . Outside these peaks ( $|\theta| > 10^{-4}$ ) the relative correction goes down approaching 0.15 at large  $\theta$ , what is below its estimation value  $\varepsilon_r \approx 0.5$ .

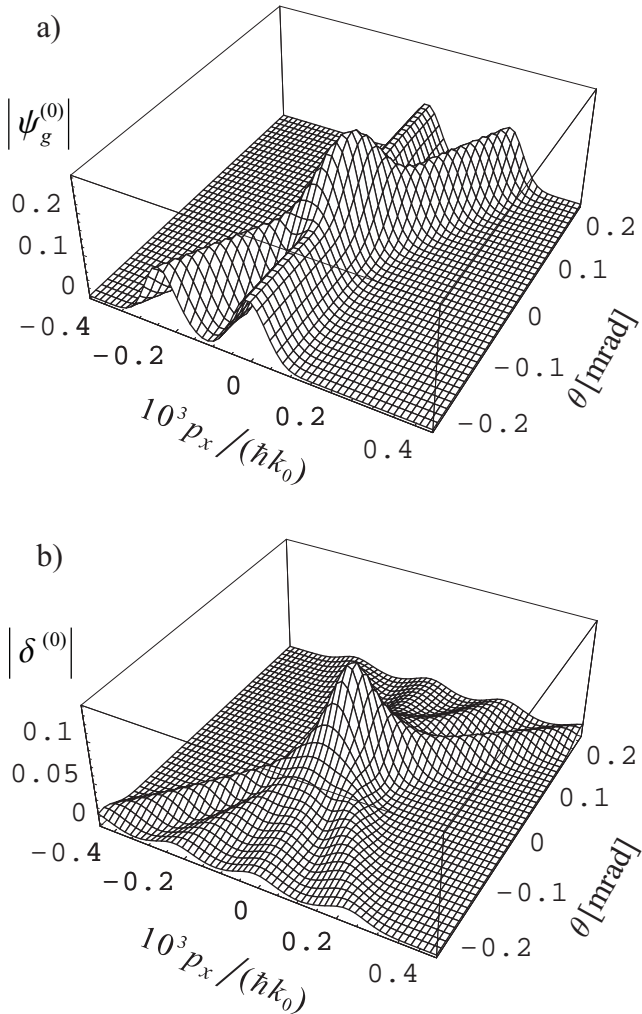


FIG. 3. Absolute values of zero-order solution  $|\psi_g^{(0)}|$  (a) and first-order correction to it  $\delta^{(0)}$  (b) as functions of the momentum component  $p_x$  and the angle  $\theta$  between  $\mathbf{k}_1$  and  $\mathbf{k}_2$ . The rest components of  $\mathbf{p}$ ,  $p_y = \hbar k_0$  and  $p_z = 0$ . The geometry of laser beams is as in the Fig. 2. The effective Rabi frequencies  $g_1 = g_2 = 10$  Hz,  $f_{12} = 0.1$  Hz.

In the worst case, e.g.,  $\mathbf{k}_m \perp \mathbf{k}_0$ ,  $\forall m \geq 1$ , one obtains more danger estimation for  $\varepsilon_r$

$$\varepsilon_r \lesssim g_\Sigma \left| \int_0^t \sin^2(g_\Sigma \tau) \exp(i\delta_\omega \tau) d\tau \right|, \quad (2.39)$$

where  $\delta_\omega = \hbar \delta_k^2 / (2M)$  stands for the minimal kinetic energy an atom can get due to transition between the laser modes. Nevertheless, the term  $\chi(\mathbf{p}, t)$  may still be treated as a perturbation if the overall effective Rabi frequency satisfies more rigorous than (2.37) condition

$$g_\Sigma \ll \delta_\omega. \quad (2.40)$$

Otherwise,  $g_\Sigma \gtrsim \delta_\omega$ , the interaction time should be limited so that  $t \ll \tau_1$ . Figure 4 shows time dependences

of  $\delta^{(0)}$ ,  $|\psi_g^{(0)}|$ , and  $|\psi_g^{(1)}|$  for two-mode object beam with  $\delta_p(\tau_1) / (\hbar \delta_k) = 0.1$  and  $g_\Sigma = 74 \delta_\omega$ . We see that in considered unfavorable configuration  $\varepsilon_r$  does not exceed 0.1 even if  $t = 0.5\tau_1$ .

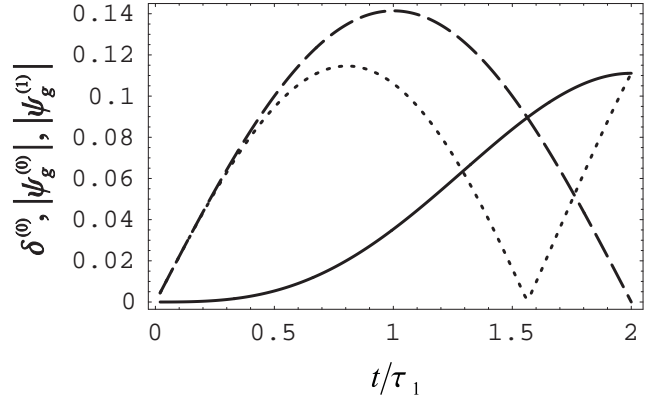


FIG. 4. Time dependences of  $\delta^{(0)}$  (solid line),  $|\psi_g^{(0)}|$  (long dashed line), and  $|\psi_g^{(1)}|$  (short dashed line) for two-mode object beam with  $\mathbf{k}_{1,2} \perp \mathbf{k}_0$ . The components of  $\mathbf{p}$ ,  $p_y = \hbar k_0$  and  $p_x = p_z = 0$ . Cartesian coordinate axes and other parameters are the same as in the Fig. 3.

In most of practical cases, however, only a small part of laser modes has a geometry leading to the condition (2.40), and the requirement (2.37) appears to be sufficient.

### III. ATOM OPTICS INTERPRETATION

#### A. General consideration

In an idealized situation, one may imagine that all atoms are initially in a pure state determined by the Gaussian profile

$$g(\mathbf{p}; \mathbf{p}_0) = \frac{L^{3/2}}{\hbar^{3/2} \pi^{3/4}} \exp \left[ \frac{-L^2(\mathbf{p} - \mathbf{p}_0)^2}{2\hbar^2} - \frac{i}{\hbar} \mathbf{p} \cdot \mathbf{r}_0 \right] \quad (3.1)$$

with mean momentum  $\mathbf{p}_0$  being close to  $\hbar \mathbf{k}_0$ , space position  $\mathbf{r}_0$ , and very small dispersion [ $L \gg \hbar / \delta_p(\tau_1)$ ]. According to the Eq. (2.7), after interaction with the laser beams within time domain  $\tau \lesssim \tau_1$  and subsequent free propagation during time  $t$  the atoms remain in pure state, and their wave function can be represented as a superposition of some useful signals  $\psi^{(s,r)}(\mathbf{p}, \tau, t; \mathbf{p}_0)$  and a background  $\psi^{(b)}(\mathbf{p}, \tau, t; \mathbf{p}_0)$ , where

$$\psi^{(\sigma)}(\mathbf{p}, \tau, t; \mathbf{p}_0) = e^{-it(\mathbf{p})t} \int d\mathbf{p}' G^{(\sigma)}(\mathbf{p}, \mathbf{p}', \tau) g(\mathbf{p}'; \mathbf{p}_0), \quad (3.2)$$

$\sigma \in \{s, r, b\}$ . The functions  $G^{(\sigma)}(\mathbf{p}, \mathbf{p}', \tau)$  are defined by Eqs. (A2). In considered case they admit of explicit analytical expressions relying on analogy with the formulas (2.27) and being exact at  $L \rightarrow \infty$ , and  $\boldsymbol{\kappa} \rightarrow \mathbf{0}$ , where  $\boldsymbol{\kappa} = \mathbf{p}_0/\hbar - \mathbf{k}_0$ . So, omitting inessential common phase factor  $\exp[-i\mathbf{k}_0 \cdot \mathbf{r}_0 - if_0\tau - (i/\hbar)E_{|g|}(0)\tau]$  we can readily ascertain that Fourier transform of  $\psi^{(r)}(\mathbf{p}, \tau, t; \mathbf{p}_0)$ ,

$$\psi_r(\mathbf{r}, \tau, t; \mathbf{p}_0) = A_r(\hbar\boldsymbol{\kappa}, \tau) \gamma_0(\mathbf{r}, \boldsymbol{\kappa}) e^{i\mathbf{k}_0 \cdot \mathbf{r} - it(\mathbf{k}_0)t}, \quad (3.3)$$

propagates like the reference beam, whereas the transform of  $\psi^{(s)}(\mathbf{p}, \tau, t; \mathbf{p}_0)$ ,

$$\begin{aligned} \psi_s(\mathbf{r}, \tau, t; \mathbf{p}_0) &= A_s(\hbar\boldsymbol{\kappa}, \tau) \\ &\times \sum_{m \geq 1} \gamma_m(\mathbf{r}, \boldsymbol{\kappa}) \frac{g_m}{g_\Sigma} e^{i\mathbf{k}_m \cdot \mathbf{r} - it(\mathbf{k}_m)t}, \end{aligned} \quad (3.4)$$

gives birth to matter wave, which inherits amplitude and phase characteristics of the object beam because  $g_m \propto \mathbf{E}_m$  as it follows from the Eq. (2.14) and definition of the Rabi frequencies  $\Omega_m$ . The last assertion also takes into account that all functions

$$\gamma_m(\mathbf{r}, \boldsymbol{\kappa}) = \frac{L^{3/2}}{\pi^{3/4}\sigma^3} \exp \left[ -\frac{L^2(\mathbf{r} - \tilde{\mathbf{r}}_t^m)^2}{2|\sigma|^4} + i\delta_\phi(\mathbf{r} - \mathbf{r}_t^m) \right], \quad (3.5)$$

used in Eqs. (3.3) and (3.4), slowly depend on  $\mathbf{r}$  within space domains  $\sim 2|\sigma|^2/L$ , each centered around the point  $\tilde{\mathbf{r}}_t^m = \mathbf{r}_t^m + \hbar(t + \tau)\boldsymbol{\kappa}/M$ , where

$$\sigma = \sqrt{L^2 + i\hbar(t + \tau)/M}, \quad (3.6)$$

$$\mathbf{r}_t^m = \mathbf{r}_0 + \frac{\hbar(\mathbf{k}_0 + \tilde{\mathbf{k}})}{2M}\tau + \frac{\hbar\mathbf{k}_m}{M}t, \quad (3.7)$$

and introduce a little phase shifts  $\delta_\phi(\mathbf{r} - \mathbf{r}_t^m)$ ,

$$\delta_\phi(\mathbf{r}) = \frac{1}{2|\sigma|^4} \left[ L^4 \mathbf{r} \cdot \boldsymbol{\kappa} + \frac{\hbar(t + \tau)(\mathbf{r}^2 - L^4\boldsymbol{\kappa}^2)}{M} \right], \quad (3.8)$$

disappearing at small  $\boldsymbol{\kappa}$  and large  $L$ .

If the overall effective Rabi frequency is chosen in agreement with the results of Sec. II D, the background, which represents itself a first-order correction to the wave function  $\psi_g^{(0)}(\mathbf{p}, \tau)$ , appears to be small at any time  $\tau \lesssim \tau_1$ . So, the states (3.3) and (3.4) being spatially separated after free propagation period  $t_{\min} = 2LM/(\hbar\Delta_k)$ , one may observe a matter wave  $\psi_s(\mathbf{r}, \tau, t; \mathbf{p}_0)$  cloning the object beam in a space-time region  $\mathcal{S} = \{(\mathbf{r}, t) : |\mathbf{r} - \tilde{\mathbf{r}}_t^m| < L, \forall m \geq 1; t > t_{\min}\}$ , where all atomic wave packets related to different modes of this beam still overlap each other. It should be noted, that  $\mathcal{S} \neq \emptyset$  only when the observation time is limited by the value  $t_{\max} = LM/[\hbar\tilde{k}\sin(\theta_{\max}/2)]$ , where  $\theta_{\max}$  characterizes the maximal divergence angle of the object beam, and  $\tilde{k} = |\tilde{\mathbf{k}}|$ . In a given context, physical sense of conditions

(2.37), (2.40) consists in the requirement to use more delicate mechanism (lower laser intensity) in order to restore more detailed information. They have a counterpart in the theory of optical holograms [see e.g., Eq. (4) in the Ref. [16]] which, in turn, is responsible for low intensity of noise in reconstructed wave.

In a more realistic case we may expect the initial atomic state to be a statistical mixture well described with the density matrix

$$\rho_{gg}(\mathbf{p}_1, \mathbf{p}_2, 0) = \int d\mathbf{p}' f(\mathbf{p}') g(\mathbf{p}_1; \mathbf{p}') g^*(\mathbf{p}_2; \mathbf{p}'), \quad (3.9)$$

where  $f(\mathbf{p})$  denotes a momentum distribution function. If this function is compatible with the condition (2.38), one can readily obtain an expression for  $\rho_{gg}(\mathbf{p}_1, \mathbf{p}_2, t)$  at any time. In the region  $\mathcal{S}$ , after rewriting into coordinate representation it takes the form

$$\rho_{gg}(\mathbf{r}_1, \mathbf{r}_2, \tau, t) = \int d\mathbf{p}' f(\mathbf{p}') \psi_s(\mathbf{r}_1, \tau, t; \mathbf{p}') \psi_s^*(\mathbf{r}_2, \tau, t; \mathbf{p}'). \quad (3.10)$$

Since  $A_s(\mathbf{p}, \tau)$  is a sharp-shape function having a narrow width  $\delta_p(\tau)$  along the vector  $\Delta_k$  [see Eq. (2.34)], the integral in Eq. (3.10) is limited in this direction. Let us assume that integration in transversal directions is also restricted within a little domain  $\sim \delta_p(\tau)$  but due to finite spectral width of  $f(\mathbf{p})$ . Then on analyzing Eq. (3.10) in the region  $|\mathbf{r}_1 - \mathbf{r}_2| \ll \hbar/\delta_p(\tau)$  under condition  $t \ll t_{\text{coh}} = M/[\tilde{k}\sin(\theta_{\max}/2)\delta_p(\tau)]$  one finds the density matrix to factorize as a product of coherent states

$$\phi(\mathbf{r}, \tau, t) = C^{1/2}(\tau) \sum_{m \geq 1} \gamma_m(\mathbf{r}, \mathbf{0}) \frac{g_m}{g_\Sigma} e^{i\mathbf{k}_m \cdot \mathbf{r} - it(\mathbf{k}_m)t}, \quad (3.11)$$

where

$$C(\tau) = \int d\mathbf{p} |A_s(\mathbf{p}, \tau)|^2 f(\mathbf{p} + \hbar\mathbf{k}_0). \quad (3.12)$$

While getting the formula (3.11) we allow for small values of phase differences  $|\delta_\phi(\mathbf{r}_1 - \mathbf{r}_t^m) - \delta_\phi(\mathbf{r}_2 - \mathbf{r}_t^n)| \ll \pi, \forall m, n \geq 1$ , appearing in the integration region at  $t \ll t_{\text{coh}}$ , whence  $\gamma_m(\mathbf{r}, \boldsymbol{\kappa}) \simeq \gamma_m(\mathbf{r}, \mathbf{0})$ . Note, compatibility of time conditions  $t_{\min} < t \ll t_{\text{coh}}$  restrains possible structure of the object beam

$$\sin(\theta_{\max}/2) \ll \frac{\hbar\Delta_k}{2L\tilde{k}\delta_p(\tau)}. \quad (3.13)$$

So, we see that the superposition of laser beams selectively acts only on those wave packets in initial representation of the atomic density matrix Eq. (3.9), whose spectra are concentrated near the vector  $\hbar\mathbf{k}_0$ , and restores a pure state (3.11) in such a way. Therefore the inhomogeneous laser radiation proves to behave like a three-dimensional hologram in respect to the incident atomic beam (impinging wave packets).

One can further establish a close relation between an atomic hologram, created in a time domain  $\tau$  and a permanent optical hologram with the thickness  $d_\tau = \hbar k_0 \tau / M$  along direction of the reading beam. Indeed, as is known from optics, the passage of reading beam through a three-dimensional hologram can be interpreted as multiple diffraction in which small waves, diffracted from different registration-media layers with equivalent transmission of light, interfere constructively to form a high intensity of reconstructed wave. The same approach can be used to describe an atom optics hologram being a light structure, inducing an optical potential through the atom-laser dipole interaction [12]. Here the role of equivalent-transmission layers in the media is performed by the equipotential surfaces. Since  $d_\tau$  is just the distance the impinging wave packet covers during time  $\tau$ , the numbers of crossed interfaces (layers or surfaces) are equal for atomic and conventional hologram. Therefore if there were no evident difference in initial and boundary conditions, the processes of wave front reconstruction would be identical in both cases.

It makes possible to classify atomic holograms as thin or thick diffractive optical elements, and use the Talbot length  $L_{\text{Talbot}}$ , i.e. the typical interval between consecutive interfaces, as a characteristic scale to distinguish between the two classes [17]. Namely the hologram can be considered as thick (three-dimensional) if  $d_\tau > L_{\text{Talbot}}$ , or in terms of time

$$\tau > L_{\text{Talbot}} M / (\hbar k_0). \quad (3.14)$$

For most of holographic setups (for instance, like that in the Fig. 2)  $L_{\text{Talbot}} \sim 2\pi/k_0$ , therefore the criterion (3.14) persists in the time domain  $\tau$  large than the period of atomic oscillations. Obviously the latter requirement is well satisfied for  $\tau \sim \tau_1$ , the time of  $\pi$  pulse, provided  $g_\Sigma$  is chosen in agreement with the condition (2.37).

### B. Diffraction efficiency

In a regime, where the background is small, we can define diffraction efficiency  $\eta$  of a hologram as overall intensity of the modes composing the reconstructed wave, provided the initial wave packet is normalized to 1

$$\eta(\tau, \mathbf{p}_0) = \int d^3 \mathbf{p} \left| \psi^{(s)}(\mathbf{p}, \tau, t; \mathbf{p}_0) \right|^2. \quad (3.15)$$

It is clear, however, that  $\eta$  depends on the shape of initial distribution as well. Therefore to be more specific let us assume the Gaussian profile (3.1) of impinging wave packet with infinitely small dispersion  $L \rightarrow \infty$ . Then, integration over  $\mathbf{p}'$  in the Eq. (3.2) becomes trivial, so that

$$\eta(\tau, \mathbf{p}_0) = \int d^3 \mathbf{p} \left| G^{(s)}(\mathbf{p}, \mathbf{p}_0, \tau) \right|^2. \quad (3.16)$$

Using approximate expressions (2.27b) and omitting negligible interference terms one readily gets from above equation

$$\eta(\tau, \mathbf{p}_0) = \eta(\tau, \xi) \simeq \frac{1}{\xi^2 + 1} \sin^2 \left( \tau g_\Sigma \sqrt{\xi^2 + 1} \right), \quad (3.17)$$

where the dimensionless parameter

$$\xi = \frac{(\mathbf{p}_0 - \hbar \mathbf{k}_0) \cdot \Delta_k}{M g_\Sigma} \quad (3.18)$$

characterizes deviation of initial atomic momentum from mean momentum of photons in the reference beam.

According to this simple formula the diffraction efficiency achieves maximum at  $\tau = \tau_n / \sqrt{\xi^2 + 1}$  and can reach 100% if  $\xi = 0$  (see Figure 5).

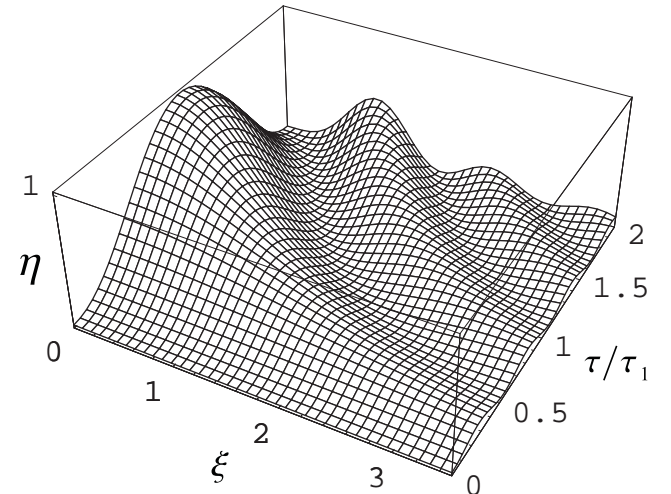


FIG. 5. Diffraction efficiency  $\eta$  of atomic hologram as a function of time domain  $\tau$  (in units of  $\pi$  pulse) and dimensionless parameter  $\xi$ .

### C. Numerical example

In the following we show two-dimensional results obtained for Na assuming experimental setup like that in the Fig. 2 (i.e., all  $\mathbf{k}_m$  are coplanar vectors and  $\tilde{\mathbf{k}} \perp \mathbf{k}_0$ ). The image to be reconstructed is a thin line of the width  $\lambda = 2\pi/k_0$  being perpendicular to laser beams plane. To decrease the bulk of computational work we reduced the number of object wave modes to 31 and set up  $\theta_{\max} = \pi/4$ . Such a field well approaches desired single line within region of size  $\sim 60\lambda$ , centered around the point  $\mathbf{r} = \mathbf{0}$ , if all laser modes going into the expression (2.5) have identical amplitudes  $\mathbf{E}_m$ , and their wave vectors  $\mathbf{k}_m$  are equidistant

$$\mathbf{k}_m = k_0 \left\{ \sin \left[ \frac{\pi(m-16)}{120} \right], -\cos \left[ \frac{\pi(m-16)}{120} \right], 0 \right\}. \quad (3.19)$$

Corresponding profile of the object beam intensity distribution  $I(x)$  is depicted in Fig. 6, where we direct Cartesian  $x$  axis along the vector  $\mathbf{k}_0 = (k_0, 0, 0)$ . The off-axis interference fringes, which are a corollary of moderate number of modes, can easily be separated from the central line and therefore do not contaminate our consideration.

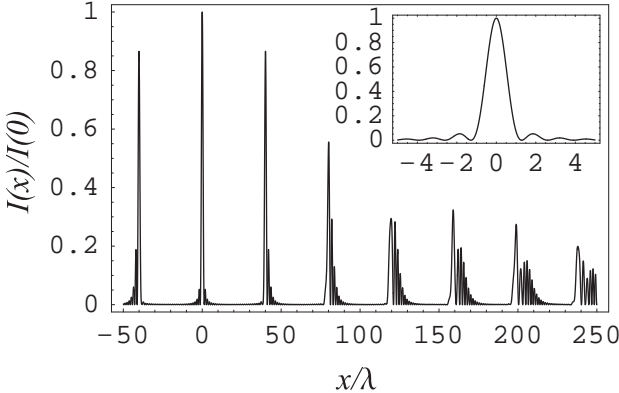


FIG. 6. Intensity  $I(x)$  of the 31-mode object wave as a function of observation point  $\mathbf{r} = (x, 0, 0)$ . The inset shows optical image of a single line  $\sim \lambda$  created in the central region  $\sim 60\lambda$ .

In numerical simulation the optical pulse duration was taken to be  $\tau_1 = 2.82 \times 10^{-2}$  c, to demonstrate the highest diffraction efficiency. The rest laser light parameters were held as follows: Rabi frequencies  $\Omega_0 = 1$  MHz and  $\Omega_m = 0.01\Omega_0$  for all  $1 \leq m \leq 31$ , detuning  $\Delta = -1$  GHz ( $\gamma/\Delta \approx 0.06$ ), the effective Rabi frequencies  $g_m = 10$  Hz,  $f_{mn} = 0.1$  Hz, and  $g_\Sigma = 55.7$  Hz. Note, that for considered laser-beams geometry  $\Delta_k = \sqrt{2}k_0 = 1.51 \times 10^5$  cm $^{-1}$  and  $\delta_k = 3.28 \times 10^3$  cm $^{-1}$ , so that the background introduces relative correction of the order  $\varepsilon_r = \delta_p(\tau_1)/(\hbar\delta_k) = 1.4 \times 10^{-2}$  and can be neglected.

The reconstruction of a real image of the object was achieved by impinging Gaussian wave packets (3.1) having spatial extension  $2L = 0.4$  cm upon the superposition of laser beams near the point

$$\mathbf{r}_0 = \left[ -\frac{\hbar k_0 \tau_1}{M}, \frac{L}{\tan(\theta_{\max}/2)} - \frac{\hbar k_0 \tau_1}{M}, 0 \right]. \quad (3.20)$$

After finishing the interaction with laser radiation these wave packets appear at a distance  $L/\tan(\theta_{\max}/2) = 0.48$  cm from the image. As a result the most intensive matter field in the imaging region may be observed after free propagation time  $t = t_{\max} \cos(\theta_{\max}/2) = 0.16$  c, which obviously lies within the limits  $t_{\min} = 9.6 \times 10^{-2}$  c and  $t_{\max} = 0.17$  c. Figure 7 shows corresponding atomic density profile  $\rho_{gg}(\mathbf{r}, \mathbf{r}, \tau_1, t)$  when the mean momentum of initial wave packet is exactly equal to  $\hbar\mathbf{k}_0$ . As it is seen from the bottom part of the plot, the atomic profile displays a good coincidence with distribution of the object

beam intensity. The diffraction efficiency calculated according to Eq. (3.15) proves to attain 98% in this case.

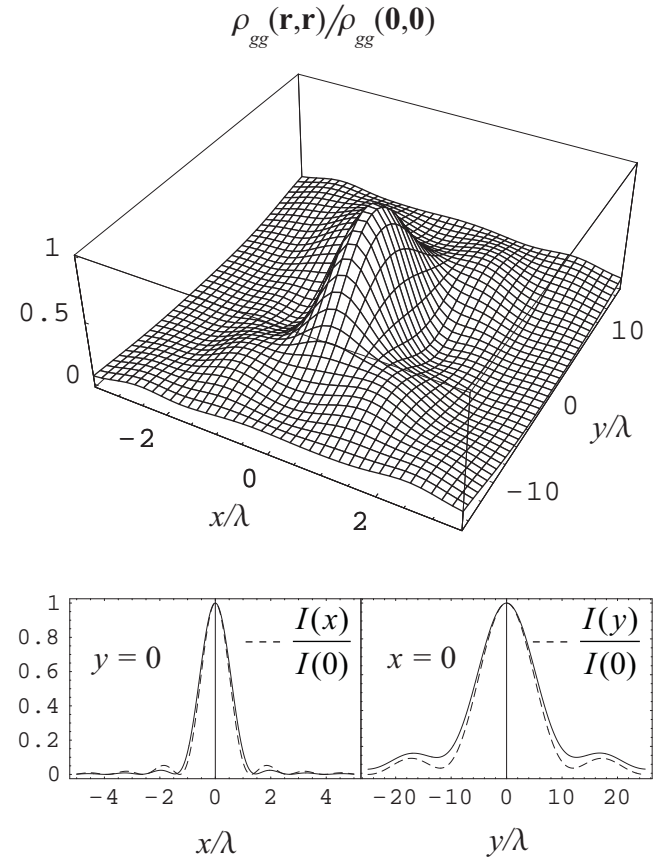


FIG. 7. Atomic density  $\rho_{gg}(\mathbf{r}, \mathbf{r}) = \rho_{gg}(\mathbf{r}, \mathbf{r}, \tau_1, t)$  as a function of observation point  $\mathbf{r} = (x, y, 0)$ . The bottom part of the plot compares atomic profile (solid lines) with the object beam intensity distributions  $I(x)$  and  $I(y)$  (dashed lines) in the planes  $y = 0$  and  $x = 0$  correspondingly.

When initial state is a statistical mixture (3.9) with momentum distribution function  $f(\mathbf{p})$  being uniform along  $x$  axis, the atomic density profile acquires a shape represented in the Fig. 8. Since condition (3.13) does not hold at chosen laser light parameters the size of reconstructed line appears to be  $\sim 4$  times wider than one might expect from coherent reading beam. Nevertheless, such image broadening is not too substantial, so that the atomic hologram can be used even in this unfavorable design.

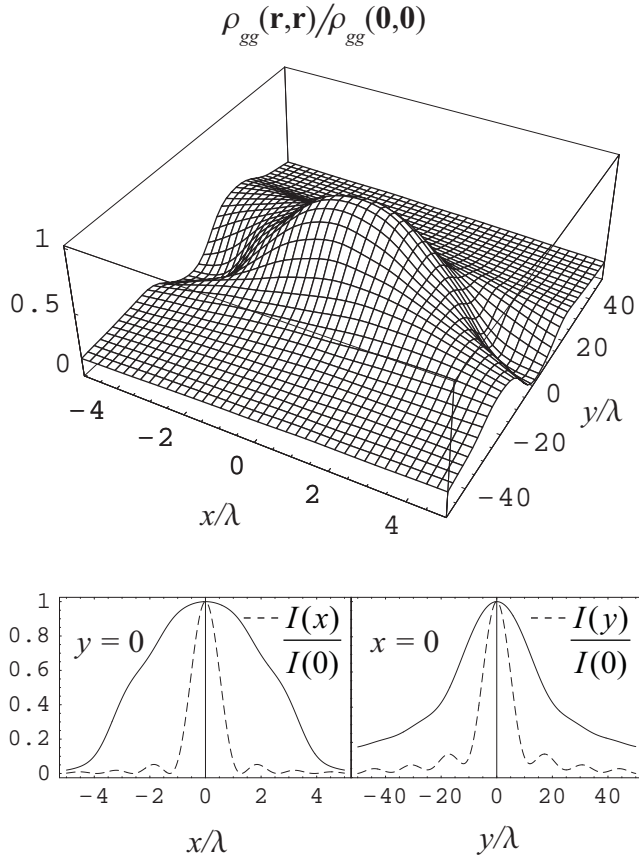


FIG. 8. Atomic density profile  $\rho_{gg}(\mathbf{r}, \mathbf{r})$  being obtained when initial state is a statistical mixture with uniform momentum distribution along  $x$  axis. Other notations are the same as in the Fig. 7.

#### IV. CONCLUSIONS

In this paper we have studied a method of driving the ultracold atom propagation using effective holograms made of laser radiation in specified time domain. We have shown that scattered atomic wave packet may inherit the features of object electromagnetic wave provided the atomic internal ground state possesses a translation invariance due to compensation of gravity with the Stern-Gerlach effect. We have established a close relation between atomic hologram created in time domain and thick optical hologram prepared in corresponding spatial region and have found a recipe how to control diffraction efficiency of such atomic hologram by means of varying the time domain. Beside adjustment of atom-laser interaction time a way to enhance diffraction efficiency has proved to consist of cooling the atomic beam so that all particles would get the same momentum as the momentum of photons in the reference wave. An extraordinary role here may be played by BEC and coherent atomic-beam generators, which are under development now [23].

The consideration has been performed for dilute atomic sample, i.e. we have not included any many-atom

interactions [24], which may lead to nonlinear atom optics effects [25] along with raising of the background. The criteria to neglect these interactions were elaborated in our previous paper [12] using mean-field approximation applied to the Maxwell-Bloch equations [26] and are well satisfied when the mean-field interaction energy per particle is much less than the typical kinetic energy of an atom. We have also neglected such possible sources of the background as spontaneous emission of photons and fluctuations of the laser frequency. While the first of these sources may be eliminated by keeping the laser detuning much bigger than the spontaneous emission rate, the second one is determined by the spectral width of two-time electromagnetic-field correlation functions [12,27] and substantially decreases if all field modes originate from one initial laser mode.

Although our scheme of atomic hologram has been developed for co-directed reading and reference beams it can readily be modified for the experimental setup with opposite propagation of the beams. On full analogy with the conventional optics such a hologram will reconstruct the conjugate object wave.

So we see that atom optics holograms appear to be a useful implement for solving some of the basic technological problems in the field of atom lithography. For instance, it will be possible to grow 3D circuitry components depositing an arbitrary multilayer picture of impurity atoms on a silicon substrate.

#### APPENDIX: GROUND-STATE GREEN FUNCTION

Here we present the first-order approximation to the ground-state component of the Green function determining time evolution of the atomic density matrix according to the formula (2.7):

$$G_{gg}(\mathbf{p}, \mathbf{p}', t) = e(t) \sum_{\sigma \in \{r, s, b\}} G^{(\sigma)}(\mathbf{p}, \mathbf{p}', t), \quad (A1)$$

where common phase multiplier  $e(t) = \exp[i\omega t - (i/\hbar)E_{|e\rangle}(0)t]$  recovers the solution (2.26) from its slow time dependence, and

$$G^{(r)}(\mathbf{p}, \mathbf{p}', t) = \mathcal{M} \left[ \phi_0^{(0)}(\mathbf{p}, \mathbf{p}', \lambda) \right], \quad (A2a)$$

$$G^{(s)}(\mathbf{p}, \mathbf{p}', t) = \sum_{m \geq 1} \mathcal{M} \left[ \phi_m^{(0)}(\mathbf{p}, \mathbf{p}', \lambda) \right], \quad (A2b)$$

$$G^{(b)}(\mathbf{p}, \mathbf{p}', t) = \sum_{m \geq 0} \mathcal{M} \left[ \phi_m^{(b)}(\mathbf{p}, \mathbf{p}', \lambda) \right]. \quad (A2c)$$

In these formulas the operator  $\mathcal{M}$  stands for inverse Laplace transformation and shift of momentum arguments

$$\mathcal{M} \left[ \phi_m^{(\sigma)}(\mathbf{p}, \mathbf{p}', \lambda) \right] \equiv 2\pi i \int_{\epsilon-i\infty}^{\epsilon+i\infty} d\lambda e^{\lambda t} \times \phi_m^{(\sigma)}(\mathbf{p} - \hbar\mathbf{k}_m, \mathbf{p}', \lambda), \quad (\text{A3})$$

$\epsilon > 0$ ,  $\sigma \in \{0, b\}$ ,  $m \geq 0$ , whereas

$$\phi_0^{(0)}(\mathbf{p}, \mathbf{p}', \lambda) = \frac{-i}{T(\mathbf{p}, \lambda)} \delta^3(\mathbf{p} + \hbar\mathbf{k}_0 - \mathbf{p}'), \quad (\text{A4a})$$

$$\phi_0^{(b)}(\mathbf{p}, \mathbf{p}', \lambda) = \frac{i}{T(\mathbf{p}, \lambda)^2} \chi(\mathbf{p}, \mathbf{p}', \lambda), \quad (\text{A4b})$$

$$\phi_m^{(\sigma)}(\mathbf{p}, \mathbf{p}', \lambda) = \frac{-g_m}{t_m(\mathbf{p}) - i\lambda} \phi_0^{(\sigma)}(\mathbf{p}, \mathbf{p}', \lambda), \quad (\text{A4c})$$

$m \geq 1$ , and expression for  $\chi(\mathbf{p}, \mathbf{p}', \lambda)$  is obtained from the formula (2.21)

$$\begin{aligned} \chi(\mathbf{p}, \mathbf{p}', \lambda) = & \sum_{m \geq 1} \left\{ \sum_{\substack{n \geq 0 \\ n \neq m}} g_m^* \phi_n^{(b)}[\mathbf{p} + \hbar(\mathbf{k}_m - \mathbf{k}_n), \mathbf{p}', \lambda] \right. \\ & + \sum_{n \geq 1} g_n \phi_m^{(b)}[\mathbf{p} + \hbar(2\mathbf{k}_0 - \mathbf{k}_n - \mathbf{k}_m), \mathbf{p}', \lambda] \\ & + \sum_{\substack{n \geq 1 \\ n \neq m}} \sum_{l \geq 0} f_{mn} \\ & \times \phi_l^{(b)}[\mathbf{p} + \hbar(\mathbf{k}_0 - \mathbf{k}_l - \mathbf{k}_m + \mathbf{k}_n), \mathbf{p}', \lambda] \left. \right\}. \end{aligned} \quad (\text{A5})$$

- [7] D. Gabor, Nature **161**, 777 (1948); Proc. R. Soc. A **197**, 454 (1949).
- [8] G. Timp, R. E. Behringer, D. M. Tennant, J. E. Cunningham, M. Prentiss, and K. K. Berggren, Phys. Rev. Lett. **69**, 1636 (1992); J. J. McClelland, R. E. Scholten, E. C. Palm, and R. J. Celotta, Science **262**, 877 (1993); R. Gupta, J. J. McClelland, Z. J. Jabbour, and R. J. Celotta, Appl. Phys. Lett. **67**, 1378 (1995).
- [9] M. Moringa, M. Yasuda, T. Kishimoto, and F. Shimizu, Phys. Rev. Lett. **77**, 802 (1996).
- [10] O. Zobay, E. V. Goldstein, and P. Meystre, Phys. Rev. A **60**, 3999 (1999).
- [11] M. Anderson, J. R. Ensher, M. R. Matthews, C. E. Wieman, and E. A. Cornell, Science **269**, 198 (1995); K. B. Davies, M.-O. Mewes, M. R. Andrews, N. J. van Druten, D. S. Durfee, D. M. Kurn, and W. Ketterle, Phys. Rev. Lett. **75**, 3969 (1995); C. C. Bradley, C. A. Sackett, J. J. Tollet, and R. Hulet, Phys. Rev. Lett. **75**, 1687 (1995).
- [12] A. V. Soroko, J. Phys. B. **30**, 5621 (1997).
- [13] M. Olshanii, N. Dekker, C. Herzog, and M. Prentiss, e-print quant-ph/9811021 (1998).
- [14] H. Kogelnik, Bell Syst. Techn. J. **48**, 2909 (1969).
- [15] P. P. Ewald, Ann. Phys. (Leipzig) **54**, 519, (1917).
- [16] V. G. Sidorovich, Zh. Tekh. Fiz. **46**, 1306, (1976).
- [17] M. K. Oberthaler, R. Affalterer, S. Bernet, C. Keller, J. Schmiedmayer, and A. Zeilinger, Phys. Rev. A **60**, 456 (1999).
- [18] A. V. Soroko, Phys. Rev. A **58**, 3963 (1998).
- [19] M.-O. Mewes, M. R. Andrews, D. M. Kurn, D. S. Durfee, C. G. Townsend, and W. Ketterle, Phys. Rev. Lett. **78**, 582 (1997).
- [20] K. Moler, D. S. Weiss, M. Kasevich, and S. Chu, Phys. Rev. A **45**, 342 (1992).
- [21] E. A. Korsunsky, D. V. Kosachiov, B. G. Matisov, and Yu. V. Rozhdestvensky, Zh. Eksp. Teor. Fiz. **103**, 396 (1993) [JETP **76**, 210 (1993)].
- [22] A. P. Kazantsev, G. A. Ryabenko, G. I. Surdutovich, and V. P. Yakovlev, Phys. Rep. **129**, 75 (1985).
- [23] R. J. C. Spreeuw, T. Pfau, U. Janicke, and M. Wilkens, Europhys. Lett. **32**, 469 (1995); H. M. Wiseman and M. J. Collett, Phys. Lett. A **202**, 246 (1995); M. Holland, K. Burnett, C. Gardiner, J. I. Cirac, and P. Zoller, Phys. Rev. A **54**, R1757 (1994); A. M. Guzman, M. Moore, and P. Meystre, *ibid.* **53**, 977 (1996); G. M. Moy, J. J. Hope, and C. M. Savage, *ibid.* **55**, 3631 (1997).
- [24] M. Lewenstein, L. You, J. Cooper, and K. Burnett, Phys. Rev. A **50**, 2207 (1994).
- [25] W. Zhang and D. F. Walls, Phys. Rev. A **49**, 3799 (1994); G. Lenz, P. Meystre, and E. M. Wright, Phys. Rev. A **50**, 1681 (1994).
- [26] Y. Castin and K. Mølmer, Phys. Rev. A **51** R3426 (1995).
- [27] B. J. Dalton and P. L. Knight, J. Phys. B. **15**, 3997 (1982).

---

- [1] A. Aspect, E. Arimondo, R. Kaiser, N. Vansteenkiste, and C. Cohen-Tannoudji, Phys. Rev. Lett. **61**, 826 (1988); J. Lawall, S. Kulin, B. Saubamea, N. Bigelow, M. Leduc, and C. Cohen-Tannoudji, *ibid.* **75**, 4194 (1995).
- [2] M. Kasevich and S. Chu, Phys. Rev. Lett. **69**, 1741 (1992); N. Davidson, H. J. Lee, M. Kasevich, and S. Chu, *ibid.* **72**, 3158 (1994); H. J. Lee, C. S. Adams, M. Kasevich, and S. Chu, *ibid.* **76**, 2658 (1996).
- [3] V. I. Balykin, V. S. Letokhov, Yu. B. Ovchinnikov, and A. I. Sidorov, Pis'ma Zh. Eksp. Teor. Fiz. **45**, 282 (1987); M. Arndt, P. Sriftgiser, J. Dalibard, and A. M. Steane, Phys. Rev. A **53**, 3369 (1996); N. Friedman, R. Ozeri, and N. Davidson, J. Opt. Soc. Am. B **16**, 1749 (1998).
- [4] P. E. Moskowitz, P. L. Gould, S. R. Atlas, and D. E. Pritchard, Phys. Rev. Lett. **51**, 370 (1983).
- [5] P. J. Martin, B. C. Oldaker, A. N. Miklich, and D. E. Pritchard, Phys. Rev. Lett. **60**, 515 (1988).
- [6] V. I. Balykin, I. I. Klimov, and V. S. Letokhov, Pis'ma Zh. Eksp. Teor. Fiz. **59**, 219 (1994); M. K. Olsen, T. Wong, S. M. Tan, and D. F. Walls, Phys. Rev. A **53**, 3358 (1996).